The Transmission-Line Matrix Method—Theory and Applications

WOLFGANG J. R. HOEFER, SENIOR MEMBER, IEEE

(*Invited Paper*)

Abstract—**This paper presents an overview of the transmission-line matrix (TLM) method of analysis, describing its historical background from Huygens's principle to modern computer formulations. The basic algorithm for simulating wave propagation in two- and three-dimensional transmission-line networks is derived. The introduction of boundaries, dielectric and magnetic materials, losses, and anisotropy are discussed in detail. Furthermore, the various sources of error and the limitations of the method are given, and methods for error correction or reduction, as well as improvements of numerical efficiency, are discussed. Finally, some typical applications to microwave problems are presented.**

I. Introduction

BEFORE THE ADVENT of digital computers, complicated electromagnetic problems which defied analytical treatment could only be solved by simulation techniques. In particular, the similarity between the behavior of electromagnetic fields, and of voltages and currents in electrical networks, was used extensively during the first half of the twentieth century to solve high-frequency field problems [2]–[4].

When modern computers became available, powerful numerical techniques emerged to predict directly the behavior of the field quantities. The great majority of these methods yield harmonic solutions of Maxwell's equations in the space or spectral domain. A notable exception is the transmission-line matrix (TLM) method of analysis which represents a true computer simulation of wave propagation in the time domain.

In this paper, the theoretical foundations of the TLM method are reviewed, its basic algorithm for simulating the propagation of waves in unbounded and bounded space is derived, and it is shown how the eigenfrequencies and field configurations of resonant structures can be determined with the Fourier transform. Sources and types of errors are discussed, and possible pitfalls are pointed out. Then, various methods of error correction are presented, and the most significant improvements to the conventional TLM approach are described. A referenced list of typical applications of the method is included as well. In the conclusion, the advantages and disadvantages of the method are summarized, and it is indicated under what circumstances it is appropriate to select the TLM method rather than other numerical techniques for solving a particular problem.

Manuscript received February 22, 1985; revised May 31, 1985.

The author is with the Department of Electrical Engineering, University of Ottawa, Ottawa, Ontario, Canada K1N 6N5.

II. Historical Background

Two distinct models describing the phenomenon of light were developed in the seventeenth century: the corpuscular model by Isaak Newton and the wave model by Christian Huygens. At the time of their conception, these models were considered incompatible. However, modern quantum physics has demonstrated that light in particular, and electromagnetic radiation in general, possess both granular (photons) and wave properties. These aspects are complementary, and one or the other usually dominates, depending on the phenomenon under study.

At microwave frequencies, the granular nature of electromagnetic radiation is not very evident, manifesting itself only in certain interactions with matter, while the wave aspect predominates in all situations involving propagation and scattering. This suggests that the model proposed by Huygens, and later refined by Fresnel, could form the basis for a general method of treating microwave propagation and scattering problems.

Indeed, Johns and Beurle [5] described in 1971 a novel numerical technique for solving two-dimensional scattering problems, which was based on Huygens's model of wave propagation. Inspired by earlier network simulation techniques [2]–[4], this method employed a Cartesian mesh of open two-wire transmission lines to simulate two-dimensional propagation of delta function impulses. Subsequent papers by Johns and Akhtarzad [6]–[16] extended the method to three dimensions and included the effect of dielectric loading and losses. Building upon the groundwork laid by these original authors, other researchers [17]–[34] added various features and improvements such as variable mesh size, simplified nodes, error correction techniques, and extension to anisotropic media.

The following section describes briefly the discretized version of Huygens's wave model which is suitable for implementation on a digital computer and forms the algorithm of the TLM method. A detailed description of this model can be found in a very interesting paper by P. B. Johns [9].

III. Huygen's Principle and Its Discretization

According to Huygens [1], a wavefront consists of a number of secondary radiators which give rise to spherical wavelets. The envelope of these wavelets forms a new

0018-9480/85/1000-0882$01.00 ©1985 IEEE

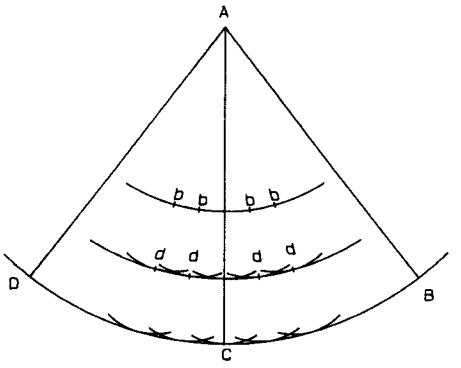

Fig. 1. Huygens's principle and formation of a wavefront by secondary wavelets.

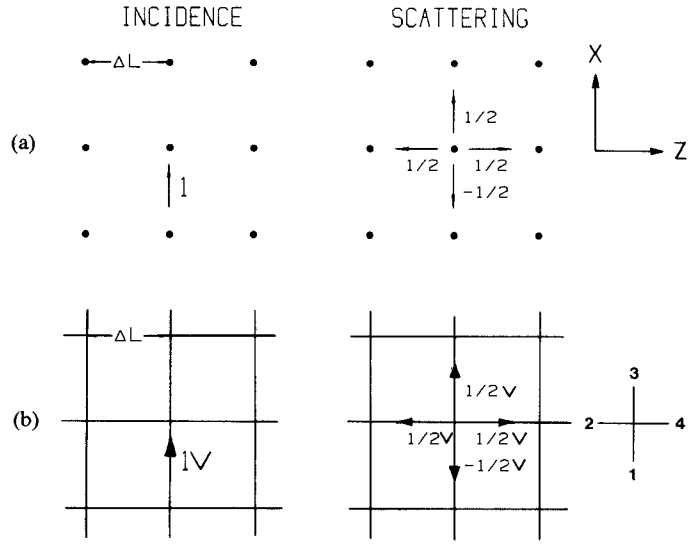

Fig. 2. The discretized Huygens's wave model (a) in two-dimensional space and (b) in an equivalent Cartesian mesh of transmission lines (after Johns [9]).

wavefront which, in turn, gives rise to a new generation of spherical wavelets, and so on (Fig. 1). In spite of certain difficulties in the mathematical formulation of this mechanism, its application nevertheless leads to an accurate description of wave propagation and scattering, as will be shown below.

In order to implement Huygens's model on a digital computer, one must formulate it in discretized form. To this end, both space and time are represented in terms of finite, elementary units Δl and Δt, which are related by the velocity of light such that

$$\Delta t = \Delta l / c. \tag{1}$$

Accordingly, two-dimensional space is modeled by a Cartesian matrix of points or nodes, separated by the mesh parameter Δl (see Fig. 2(a)). The unit time Δt is then the time required for an electromagnetic pulse to travel from one node to the next.

Assume that a delta function impulse is incident upon one of the nodes from the negative x-direction. The energy in the pulse is unity. In accordance with Huygen's principle, this energy is scattered isotropically in all four directions, each radiated pulse carrying one fourth of the incident energy. The corresponding field quantities must then be $1/2$ in magnitude. Furthermore, the reflection coefficient "seen" by the incident pulse must be negative in order to satisfy the requirement of field continuity at the node.

This model has a network analog in the form of a mesh of orthogonal transmission lines, or transmission-line matrix (Fig. 2(b)), forming a Cartesian array of shunt nodes which have the same scattering properties as the nodes in Fig. 2(a). It can be shown that there is a direct equivalence between the voltages and currents on the line mesh and the electric and magnetic fields of Maxwell's equations [5].

Consider the incidence of a unit Dirac voltage-impulse on a node in the TLM mesh of Fig. 2(b). Since all four branches have the same characteristic impedance, the reflection coefficient "seen" by the incident impulse is indeed $-1/2$, resulting in a reflected impulse of -0.5 V and three transmitted impulses of $+0.5$ V.

The more general case of four impulses being incident on the four branches of a node can be obtained by superposition from the previous case. Hence, if at time $t = k\,\Delta t$, voltage impulses ${}_kV_1^i$, ${}_kV_2^i$, ${}_kV_3^i$, and ${}_kV_4^i$ are incident on lines 1–4, respectively, on any junction node, then the total voltage impulse reflected along line n at time $(k+1)\,\Delta t$ will be

$${}_{k+1}V_n^r = \frac{1}{2}\left[\sum_{m=1}^{4} {}_kV_m^i\right] - {}_kV_n^i. \tag{2}$$

This situation is conveniently described by a scattering matrix equation [7] relating the reflected voltages at time $(k+1)\,\Delta t$ to the incident voltages at the previous time step $k\,\Delta t$

$${}_{k+1}\begin{pmatrix} V_1 \\ V_2 \\ V_3 \\ V_4 \end{pmatrix}^r = 1/2 \begin{pmatrix} -1 & 1 & 1 & 1 \\ 1 & -1 & 1 & 1 \\ 1 & 1 & -1 & 1 \\ 1 & 1 & 1 & -1 \end{pmatrix} \times {}_k\begin{pmatrix} V_1 \\ V_2 \\ V_3 \\ V_4 \end{pmatrix}^i. \tag{3}$$

Furthermore, any impulse emerging from a node at position (z, x) in the mesh (reflected impulse) becomes automatically an incident impulse on the neighboring node. Hence

$$\begin{aligned} {}_{k+1}V_1^i(z,x) &= {}_{k+1}V_3^r(z,x-1) \\ {}_{k+1}V_2^i(z,x) &= {}_{k+1}V_4^r(z-1,x) \\ {}_{k+1}V_3^i(z,x) &= {}_{k+1}V_1^r(z,x+1) \\ {}_{k+1}V_4^i(z,x) &= {}_{k+1}V_2^r(z=1,x). \end{aligned} \tag{4}$$

Consequently, if the magnitudes, positions, and directions of all impulses are known at time $k\,\Delta t$, the corresponding values at time $(k+1)\,\Delta t$ can be obtained by operating (3) and (4) on each node in the network. The impulse response of the network is then found by initially fixing the magni-

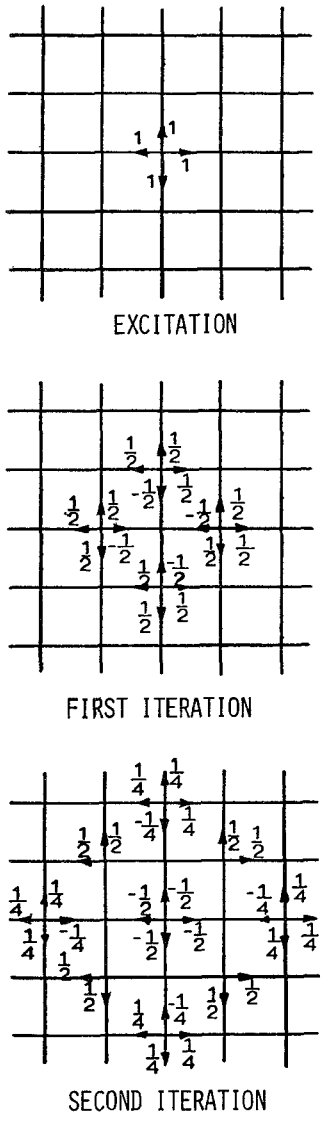

Fig. 3. Three consecutive scatterings in a two-dimensional TLM network excited by a Dirac impulse.

tudes, directions, and positions of all impulses at $t = 0$ and then calculating the state of the network at successive time intervals.

The scattering process described above forms the basic algorithm of the TLM method. Three consecutive scatterings are shown in Fig. 3, visualizing the spreading of the injected energy across the two-dimensional network.

This sequence of events closely resembles the disturbance of a pond due to a falling drop of water. However, there is one obvious difference, namely the discrete nature of the TLM mesh which causes dispersion of the velocity of the wavefront. In other words, the velocity of a signal component in the mesh depends on its direction of propagation as well as on its frequency.

In order to appreciate the importance of this dispersion, note that the process in Fig. 3 depicts a short episode of the response of the TLM network to a single impulse which contains all frequencies. Thus, harmonic solutions to a problem are obtained from the impulse response via the

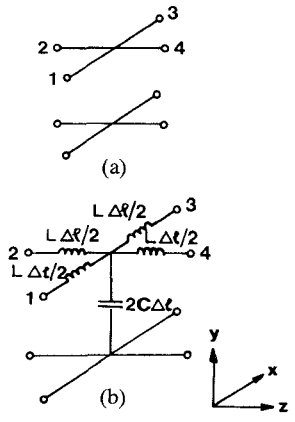

Fig. 4. The building block of the two-dimensional TLM network. (a) Shunt node. (b) Equivalent lumped-element model.

Fourier transform. Accurate solutions will be obtained only at frequencies for which the dispersion effect can be neglected. This aspect will be discussed in Section IV.

The TLM mesh can be extended to three dimensions, leading to a rather complex network containing series as well as shunt nodes. Each of the six field components is simulated by a voltage or a current in that mesh. Three-dimensional TLM networks will be discussed in Section V.

IV. The Two-Dimensional TLM Method

A. Wave Properties of the TLM Network

The basic building block of a two-dimensional TLM network is a shunt node with four sections of transmission lines of length $\Delta l/2$ (see Fig. 4(a)). Such a configuration can be approximated by the lumped-element model shown in Fig. 4(b). Comparing the relations between voltages and currents in the equivalent circuit with the relations between the H_z-, H_x-, and E_y-components of a TE_{m0} wave in a rectangular waveguide, the following equivalences can be established [5]:

$$\begin{aligned} E_y &\equiv V_y \qquad -H_z \equiv (I_{x3} - I_{x1}) \\ -H_x &\equiv (I_{z2} - I_{z4}) \quad \mu \equiv L \quad \epsilon \equiv 2C. \end{aligned} \tag{5}$$

For elementary transmission lines in the TLM network, and for $\mu_r = \epsilon_r = 1$, the inductance and capacitance per unit length are related by

$$1/\sqrt{LC} = 1/\sqrt{\epsilon_0 \mu_0} = c \tag{6}$$

where $c = 3 \times 10^8$ m/s.

Hence, if voltage and current waves on each transmission-line component travel at the speed of light, the complete network of intersecting transmission lines represents a medium of relative permittivity twice that of free space. The means that as long as the equivalent circuit in Fig. 4 is valid, the propagation velocity in the TLM mesh is $1/\sqrt{2}$ the velocity of light.

Note that the dual nature of electric and magnetic fields also allows us to simulate, for example, the longitudinal

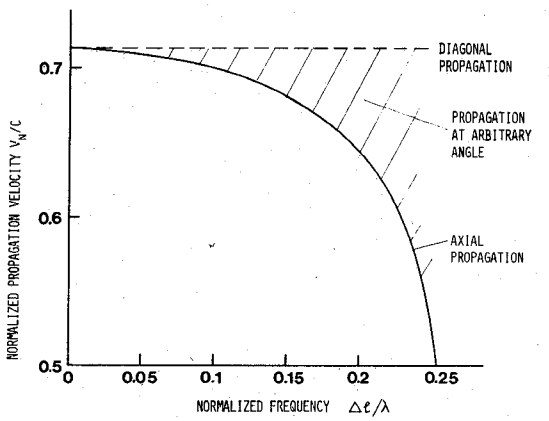

Fig. 5. Dispersion of the velocity of waves in a two-dimensional TLM network (after Johns and Beurle [5]).

magnetic field of TE modes by the network voltage, while the network currents simulate the transverse electric-field components. Whatever the relationship between field and network variables, the wave properties of the mesh, which will be discussed next, remain the same. Considering the mesh as a periodic structure, Johns and Beurle [5] calculate the following dispersion relation for propagation along the main mesh axes:

$$\sin(\beta_n \Delta l/2) = \sqrt{2}\sin[\omega \Delta l/(2c)] \tag{7}$$

where β_n is the propagation constant in the network. The resulting ratio of velocities on the matrix and in free space, $v_n/c = \omega/(\beta_n c)$, is shown in Fig. 5. It appears that a first cutoff occurs for $\Delta l/\lambda = 1/4$ (λ is the free-space wavelength). However, no cutoff occurs in the diagonal direction, where the velocity is frequency-independent, while in intermediate directions, the velocity ratio lies somewhere between the two curves shown in Fig. 5.

In conclusion, the TLM network simulates an isotropic propagating medium only as long as all frequencies are well below the network cutoff frequency, in which case the network propagation velocity may be considered constant and equal to $c/\sqrt{2}$.

B. Representation of Lossless and Lossy Boundaries

Electric and magnetic walls are represented by short and open circuits, respectively, at the appropriate positions in the TLM mesh. To ensure synchronism, they must be placed halfway between two nodes. In practice, this is achieved by making the mesh parameter Δl an integer fraction of the structure dimensions. Curved walls are represented by piecewise straight boundaries as shown in Fig. 6.

In the computation, the reflection of an impulse at a magnetic or electric wall is achieved by returning it, after one unit time step Δt, with equal or opposite sign to its boundary node of origin.

Lossy boundaries can be represented in the same way as lossless boundaries, with the difference that the reflection coefficient in each boundary branch is now

$$\rho = (R-1)/(R+1) \tag{8}$$

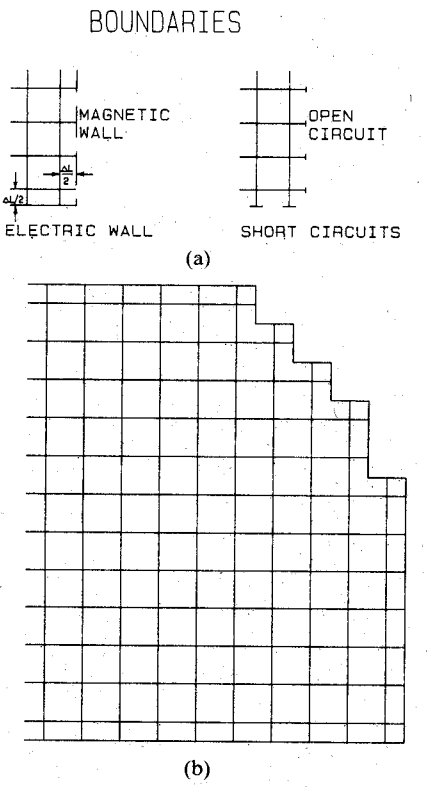

Fig. 6. Representation of boundaries in the TLM mesh. (a) Electric and magnetic walls. (b) Curved wall represented by a piecewise straight boundary.

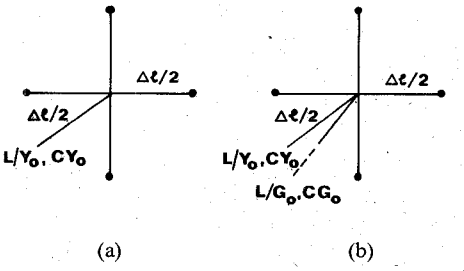

Fig. 7. Simulation of permittivity and losses. (a) Permittivity stub. (b) Permittivity stub and loss stub.

instead of unity. R is the normalized surface resistance of the boundary.

For a good but imperfect conductor of conductivity σ, the reflection coefficient ρ is approximately

$$\rho \simeq -1+2[\epsilon_0 \omega/(2\sigma)]^{1/2}. \tag{9}$$

Note that since ρ depends on the frequency ω, the loss calculations are accurate only for that frequency which has been selected in determining ρ.

C. Representation of Dielectric and Magnetic Materials

The presence of dielectric or magnetic material (for example, in partial dielectric or magnetic loading of a waveguide) can be taken into account by loading inside nodes with reactive stubs of appropriate characteristic impedance and a length equal to half the mesh spacing [7], as shown in Fig. 7(a). For example, if the network voltage

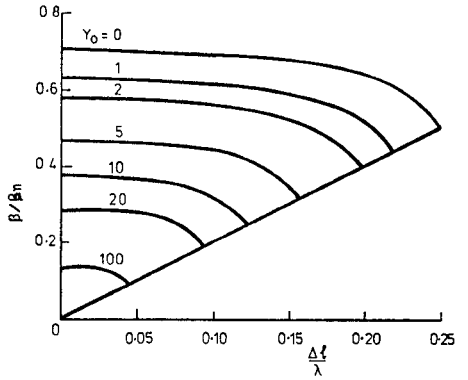

Fig. 8. Dispersion of the velocity of waves in a two-dimensional stub-loaded TLM network with the characteristic admittance of the reactive stubs as a parameter (after Johns [7]).

simulates an electric field, an open-circuited shunt stub of length $\Delta l/2$ will produce the effect of additional capacity at the nodes. This reduces the phase velocity in the structure and, at the same time, satisfies the boundary conditions at the air–dielectric interface [7]. At low frequencies, the velocity of waves in the stub-loaded TLM mesh is given by

$$v_n^2 = 0.5c^2/(1+Y_0/4) \tag{10}$$

where c is the free-space velocity, and Y_0 is the characteristic admittance of the stubs, normalized to the admittance of the main network lines. Note that the velocity in the network is now made variable by altering the single constant Y_0. The relationship between ϵ_r of the simulated space and Y_0 is

$$\epsilon_r = 2(1+Y_0/4). \tag{11}$$

The velocity characteristic along the main axes of the stub-loaded network is shown in Fig. 8 for various values of Y_0. Again, for relatively low frequencies, the mesh velocity is practically the same in all directions.

In cases where the voltage on the TLM mesh represents a magnetic field, the open shunt stubs describe a permeability. The velocity of waves in a magnetically loaded medium will be simulated correctly by such a mesh. However, the interface conditions are not satisfied, and a correction must be introduced in the form of local reflection and transmission coefficients at the interface between the media, as described in [7].

D. Description of Dielectric Losses

Losses in a dielectric can be accounted for in two different ways. One can either consider the TLM mesh to consist of lossy transmission lines, or one can load the nodes of a lossless mesh with so-called loss-stubs (Fig. 7(b)).

In the first case, the magnitude of each pulse is reduced by an appropriate amount while traveling from one node to the next, and the ensuing change in velocity is accounted for by increasing the time required to reach the next node [8]. This method is particularly suited for homogeneous structures.

In the second case, each node is resistively loaded with a matched transmission line of appropriate characteristic admittance G_0, extracting energy from each node at every iteration [10]. This technique is more suitable for inhomogeneous structures since it describes the interface conditions as well as the loss mechanism.

The normalized admittance of the loss-stub is related to the conductivity σ of the lossy medium by

$$G_0 = \sigma \Delta l (\mu_0/\epsilon_0)^{1/2}. \tag{12}$$

E. Computation of the Frequency Response of a Structure

The previous sections have described how the wave properties of two-dimensional unbounded and bounded space can be simulated by a two-dimensional mesh of transmission lines, and how the impulse response of such a mesh can be computed by iteration of (3) and (4). Any node (or several nodes) may be selected as input and/or output points. The output function is an infinite series of discrete impulses of varying magnitude, representing the response of the system to an impulsive excitation (see Fig. 12). The output corresponding to any other input may be obtained by convolving it with this impulse response.

Of particular interest is the response to a sinusoidal excitation which is obtained by taking the Fourier transform of the impulse response. Since the latter is a series of delta functions, the Fourier integral becomes a summation, and the real and imaginary parts of the output spectrum are

$$\mathrm{Re}\,[F(\Delta l/\lambda)] = \sum_{k=1}^{N} {}_kI \cos(2\pi k \Delta l/\lambda) \tag{13}$$

$$\mathrm{Im}\,[F(\Delta l/\lambda)] = \sum_{k=1}^{N} {}_kI \sin(2\pi k \Delta l/\lambda) \tag{14}$$

where $F(\Delta l/\lambda)$ is the frequency response, ${}_kI$ is the value of the output response at time $t = k\Delta l/c$, and N is the total number of time intervals for which the calculation has been made, henceforth called the "number of iterations."

In the case of a closed structure, this frequency response represents its mode spectrum. A typical example is Fig. 9(a), which shows the cutoff frequencies of the modes in a WR-90 waveguide.

Note that, as in a real measurement, the position of input and output points as well as the nature of the field component under study will affect the magnitudes of the spectral lines. For example, if input and output nodes are situated close to a minimum of a particular mode field, the corresponding eigenfrequency will not appear in the frequency response. This feature can be used either to suppress or enhance certain modes.

F. Computation of Fields and Impedances

Since the network voltages and currents are directly proportional to field quantities in the simulated structure, the TLM method also yields the field distribution. In order to obtain the configuration of a particular mode, its eigen-

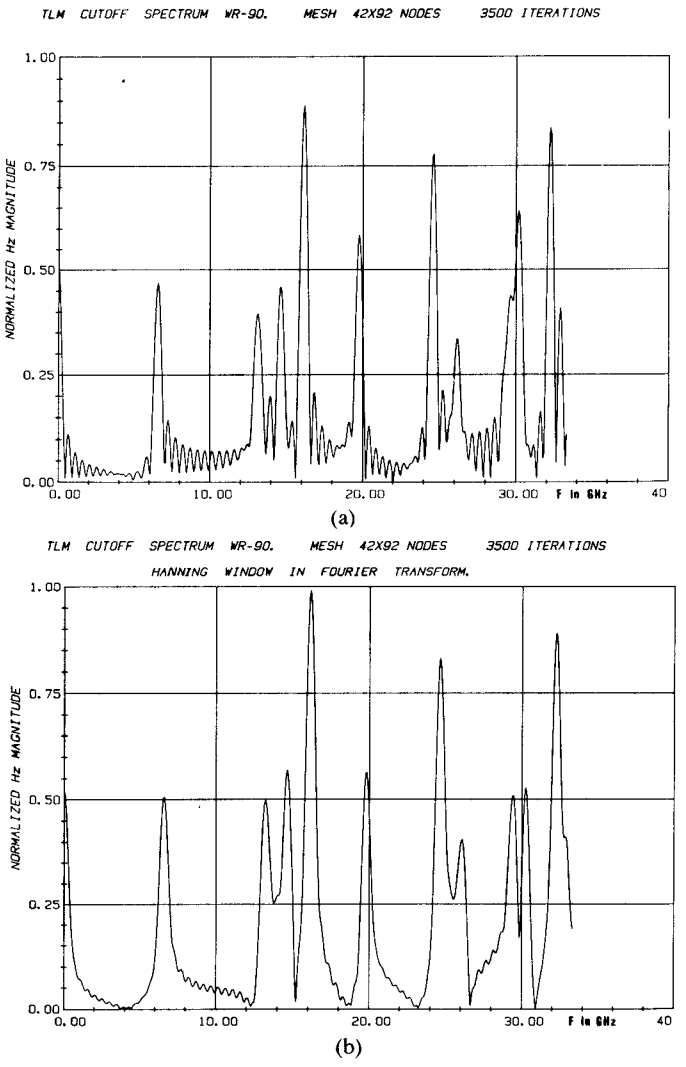

Fig. 9. Typical output from a two-dimensional TLM program. (a) Cutoff spectrum of a WR-90 waveguide. (b) The same spectrum after convolution of the output impulse function with a Hanning window (TLM) mesh: 42×92 nodes, 3500 iterations).

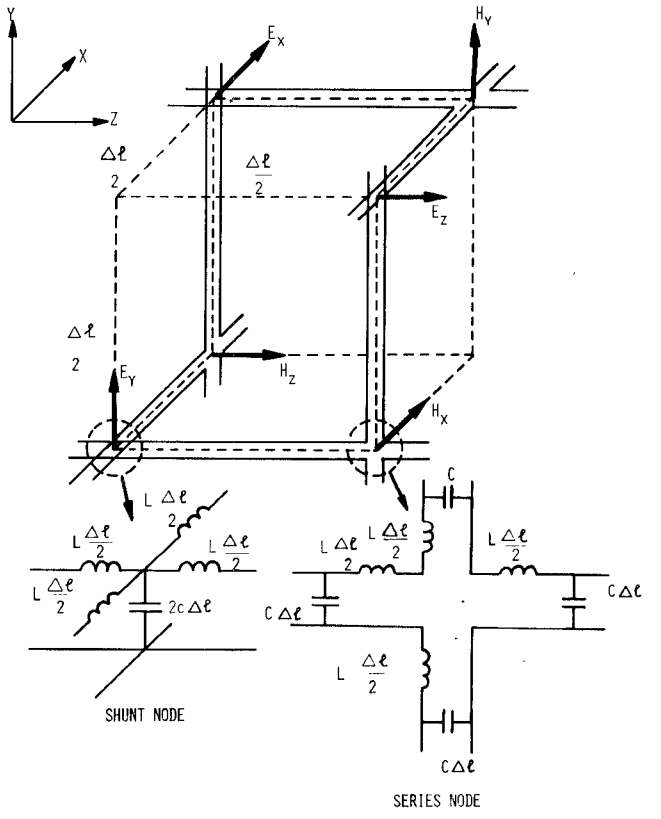

Fig. 10. The three-dimensional TLM cell featuring three series and three shunt nodes.

frequency must be computed first. Then the Fourier transform of the network variable representing the desired field component is computed at each node during a second run. In this process, (13) and (14) are computed for each node, with $\Delta l/\lambda$ corresponding to the eigenfrequency of the mode. The field between nodes can be obtained by interpolation techniques.

Impedances can, in turn, be obtained from the field quantities. Local field impedances can be found directly as the ratio of voltages and currents at a node, while impedances defined on the basis of particular field integrals (such as the voltage–power impedance in a waveguide) are computed by stepwise integration of the discrete field values. This procedure is identical to that used in finite-element and finite-difference methods of analysis.

V. The Three-Dimensional TLM Method

The two-dimensional method described above can be extended to three dimensions at the expense of increased complexity [10] to [15]. In order to simultaneously describe all six field components in three-dimensional space, the basic shunt node must be replaced by a hybrid TLM cell consisting of three shunt and three series nodes as shown in Fig. 10. The side of the cell is $\Delta l/2$. The voltages at the three series nodes represent the three electric-field components, while the currents at the series nodes represent the magnetic-field components.

The wave properties of the three-dimensional mesh are similar to that of its two-dimensional counterpart with the difference that the low-frequency velocity is now $c/2$ instead of $c/\sqrt{2}$ [15].

Boundaries are simulated by short-circuiting shunt nodes (electric wall) or open-circuiting shunt nodes (magnetic wall) situated on a boundary. Wall losses are included by introducing imperfect reflection coefficients.

Magnetic and dielectric materials may be introduced by adding short-circuited $\Delta l/2$ series stubs at the series nodes and open-circuited $\Delta l/2$ shunt stubs at the shunt nodes, respectively. Furthermore, losses are taken into account by resistively loading the shunt nodes in the network (see Fig. 11). Even anisotropic materials may be simulated by introducing at each of the three series or shunt nodes of a cell a stub with a different characteristic admittance [17]. Finally, losses as well as permittivities and permeabilities can be varied in space and in time by controlling the admittances of the dissipative and reactive stubs. The relationships between material parameters and stub admittances are the same as in the two-dimensional case.

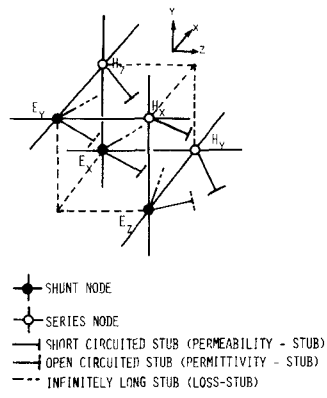

Fig. 11. Simulation of permittivity, permeability, and losses in a three-dimensional TLM network (after Akhtarzad [13]).

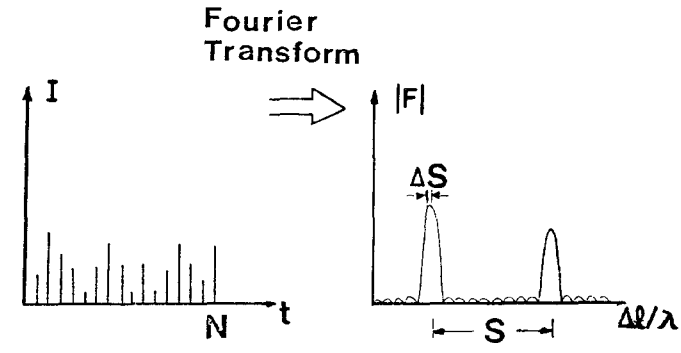

Fig. 12. (a) Truncated output impulse response and (b) resulting truncation error in the frequency domain.

The impulse response of a three-dimensional network is found in the same way as in the two-dimensional case, and everything that has been said about the computation of eigenfrequencies, fields, and impedances, applies here as well.

VI. Errors and Their Correction

Like all other numerical techniques, the TLM method is subject to various sources of error and must be applied with caution in order to yield reliable and accurate results. The main sources of error are due to the following circumstances:

a) The impulse response must be truncated in time.
b) The propagation velocity in the TLM mesh depends on the direction of propagation and on the frequency.
c) The spatial resolution is limited by the finite mesh size.
d) Boundaries and dielectric interfaces cannot be aligned in the 3-D TLM model.

The resulting errors will be discussed below, and ways of eliminating or, at least, significantly reducing these errors will be described.

A. Truncation Error

The need to truncate the output impulse function leads to the so-called truncation error: Due to the finite duration of the impulse response, its Fourier transform is not a line spectrum but rather a superposition of $\sin x/x$ functions (Gibbs's phenomenon) which may interfere with each another such that their maxima are slightly shifted. The resulting error in the eigenfrequency, or truncation error, is given by

$$E_T \leqq \Delta S/(\Delta l/\lambda_c) = 3\lambda_c/(SN^2\pi^2\Delta l) \qquad (15)$$

where N is the number of iterations and S is the distance in the frequency domain between two neighboring spectral peaks (see Fig. 12).

This expression shows that the truncation error decreases with increasing separation S and increasing number of iterations N. It is thus desirable to suppress all unwanted modes close to the desired mode by choosing appropriate input and output points in the TLM network. Another technique, proposed by Saguet and Pic [20], is to use a Hanning window in the Fourier transform, resulting in a considerable attenuation of the sidelobes.

In this process, the output impulse response is first convolved with the Hanning profile

$$f_k(k) = 0.5(1+\cos \pi k/N), \qquad k = 1,2,3,\cdots,N \qquad (16)$$

where k is the iteration variable or counter. The filtered impulse response is then Fourier transformed. The resulting improvement can be appreciated by comparing Figs. 9(a) and 9(b).

Finally, the number of iterations may be made very large, but this leads to increased CPU time. It is recommended that the number of iterations be chosen such that the truncation error given by (16) is reduced to a fraction of a percent and can be neglected.

B. Velocity Error

If the wavelength in the TLM network is large compared with the network parameter Δl, it can be assumed that the fields propagate with the same velocity in all directions. However, when the wavelength decreases, the velocity depends on the direction of propagation (see Fig. 5). At first glance, the resulting velocity error can be reduced only by choosing a very dense mesh, unless propagation occurs essentially in an axial direction (e.g., rectangular waveguide), in which case the error can be corrected directly using the dispersion relation (7). Fortunately, the velocity error responds to the same remedial measures as the coarseness error (which will be described next), and it therefore does not need to be corrected separately.

C. Coarseness Error

The coarseness error occurs when the TLM mesh is too coarse to resolve highly nonuniform fields as can be found at corners and wedges. This error is particularly cumbersome when analyzing planar structures which contain such regions. A possible but impractical measure would be to choose a very fine mesh. However, this would lead to large memory requirements, particularly for three-dimensional

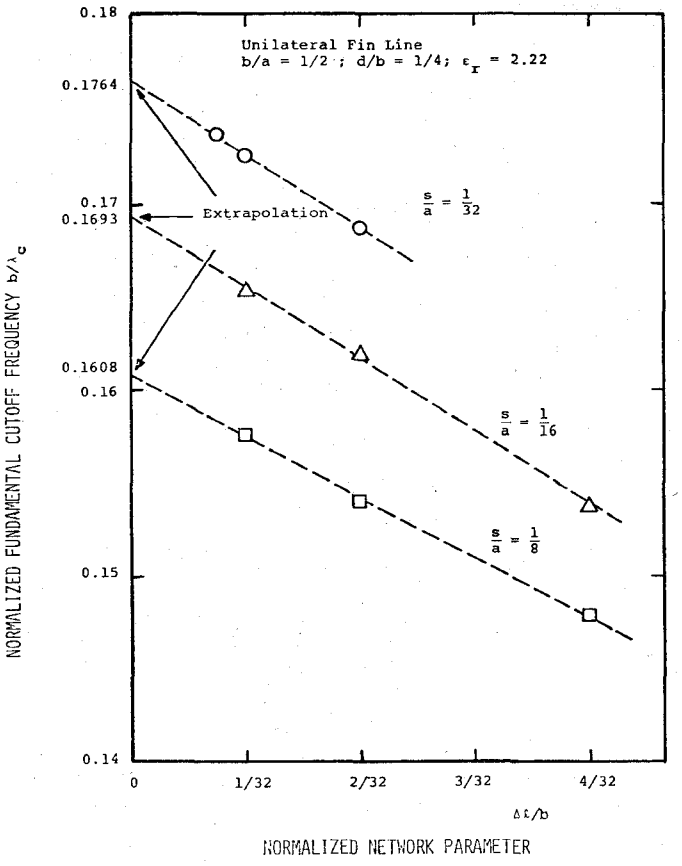

Fig. 13. Elimination of coarseness error by linear extrapolation of results obtained with TLM meshes of different parameter $\Delta l/b$ (after Shih and Hoefer [25]).

problems. A better response is to introduce a network of variable mesh size to provide higher resolution in the nonuniform field region [27]–[29]. This approach is described in the next section; however, it requires more complicated programming. Yet another approach, proposed by Shih and Hoefer [25], is to compute the structure response several times using coarse meshes of different mesh parameter Δl, and then to extrapolate the obtained results to $\Delta l = 0$ as shown in Fig. 13.

Both measures effectively reduce the error by one order of magnitude and simultaneously correct the velocity error.

D. Misalignment of Dielectric Interfaces and Boundaries in Three-Dimensional Inhomogeneous Structures

Due to the particular way in which boundaries are simulated in a three-dimensional TLM network, dielectric interfaces appear halfway between nodes, while electric and magnetic boundaries appear across such nodes. This can be a problem when simulating planar structures such as microstrip or finline. In the TLM model, the dielectric either protrudes or is undercut by $\Delta l/2$, as shown in Fig. 14. Unless the resulting error is acceptable, one must make two computations, one with recessed and one with protruding dielectric, and take the average of the results. The problem does not occur in a variation of the three-dimensional TLM method involving an alternative node configuration proposed by Saguet and Pic [31], and described in the next section.

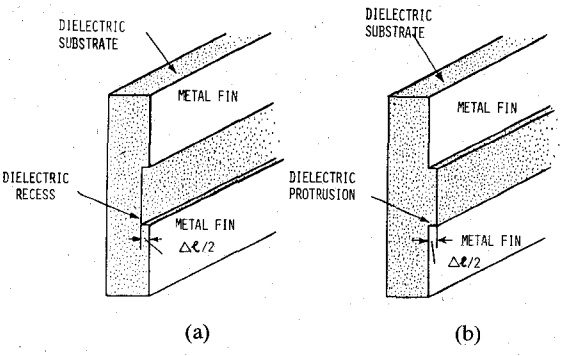

Fig. 14. Misalignment of conducting boundaries and dielectric interfaces in the three-dimensional TLM simulation of planar structures (after Shih [26]).

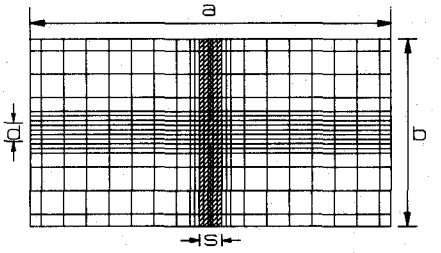

Fig. 15. Two-dimensional TLM network with variable mesh size for the computation of cutoff frequencies of finlines (after Saguet and Pic [28]).

VII. Variations of the TLM Method

A number of modifications of the conventional TLM method have been proposed over the last few years with the aim of reducing errors, memory requirements, and CPU time. Some of them have already been mentioned, such as the introduction of a Hanning window [20], and extrapolation from coarse mesh calculations [21], [25]. Some effort has also been directed towards improving the efficiency of programing techniques [24].

In the following, three other interesting and significant innovations will be discussed briefly.

A. TLM Networks with Nonuniform Mesh

In order to ensure synchronism, the conventional TLM network uses a uniform mesh parameter throughout. This can lead to considerable numerical expenditure if the structure contains sharp corners or fins producing highly nonuniform fields and thus demands a high density mesh. Saguet and Pic [28] and Al-Mukhtar and Sitch [29] have independently proposed ways to implement irregularly graded TLM meshes which, as in the finite-element method, allow the network to adapt its density to the local nonuniformity of the fields. Fig. 15 shows such a network as proposed by Saguet and Pic [28] for the computation of cutoff frequencies in a finline. Note, however, that the size of the mesh cells is not arbitrary as in the case of finite elements; the length of each side is an odd integer multiple P of the smallest cell length in the network. To keep the

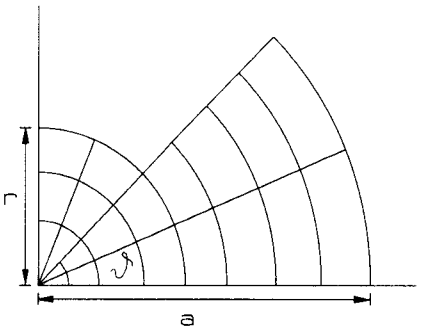

Fig. 16. A radial TLM mesh for the treatment of circular ridged waveguides (after Al-Mukhtar and Sitch [29]).

velocity of traveling impulses the same in all branches, the inductivity per unit length of the longer mesh lines is increased by a factor P while their capacity per unit length is reduced by $1/P$. This, in turn, increases their characteristic impedance by a factor P, and the scattering matrix of nodes connecting cells of different size must be modified accordingly.

To preserve synchronism, impulses traveling on longer branches are kept in store for P iterations before being reinjected at the next node.

For the configuration shown in Fig. 15, Saguet and Pic found that computing time was reduced between 3.5 and 5 times over a uniform mesh, depending on the relative size of the larger cells.

A different approach has been proposed by Al-Mukhtar and Sitch [27], [29]. They describe two possible ways to modify the characteristics of mesh elements in order to ensure synchronism, one involving the insertion of series stubs between nodes and loading of nodes by shunt stubs, the other involving modification of inductivity and capacity per unit length in such a way that propagation velocity in a branch becomes proportional to its length. The work by Al-Mukhtar and Sitch also covers the representation of radial meshes (see Fig. 16) as well as three-dimensional inhomogeneous structures. They report an economy of 45 percent in computer expenditure for a two-dimensional ridged waveguide problem, and a 40-percent reduction in storage and an 80-percent reduction in run time for a three-dimensional finline problem thanks to mesh grading.

B. A Punctual Node for Three-Dimensional TLM Networks

Conventional three-dimensional TLM networks require three shunt and three series nodes for the representation of one single cell (see Fig. 10). Saguet and Pic [31] have proposed an alternative method of interconnection. Representation of the short transmission-line sections by two rather than three lumped elements (see Fig. 17) makes it possible to realize both shunt and series connections in one point, resulting in a punctual node with 12 branches. This node is equivalent to a cell, such as that in Fig. 10, in which the inner connections have been eliminated. Losses and dielectric or magnetic loading can be simulated with stubs in the same way as discussed earlier.

This new node representation reduces, according to Saguet and Pic [31], the computation time by about 30 percent. By employing both the punctual node and variable mesh size in a three-dimensional program, Saguet [32] has computed the resonant frequencies of a finline cavity 35 times faster than with a program based on the traditional TLM method.

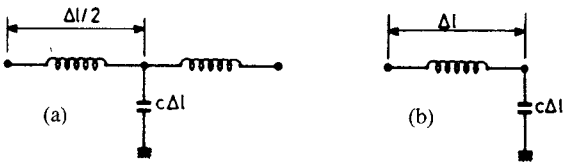

Fig. 17. Alternative lumped-element network for the two-dimensional shunt node. (a) Classical representation. (b) Representation proposed by Saguet and Pic [31].

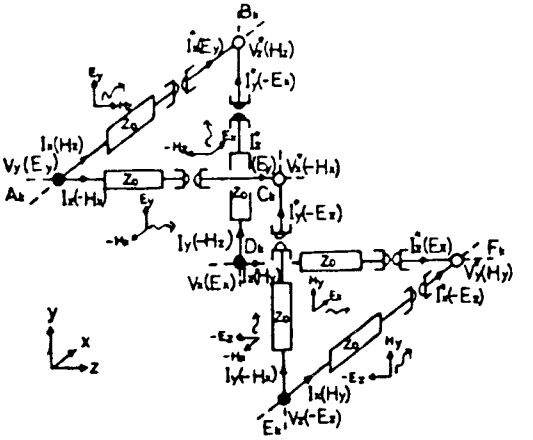

Fig. 18. Alternative network for three-dimensional TLM analysis proposed by Yoshida *et al.* [33]. (a) Equivalent circuit of an alternative three-dimensional TLM cell. (b) Definition of gyrators in (a): 1) positive gyrator, 2) negative gyrator.

C. Alternative Network Simulating Maxwell's Equations

Yoshida, Fukai, and Fukuoka [19], [23], [30], [33] have described a network similar to the TLM mesh, differing only in the way the basic cell element has been modeled. Instead of series and shunt nodes, this network contains so-called electric and magnetic nodes which are both "shunt-type nodes": while at the electric node, the voltage variable represents an electric field, it symbolizes a magnetic field at the magnetic node. The resulting ambivalence in the nature of the network voltage and current must be removed by inserting gyrators between the two types of nodes, as shown in Fig. 18. The wave properties of this network are identical with that of the conventional TLM

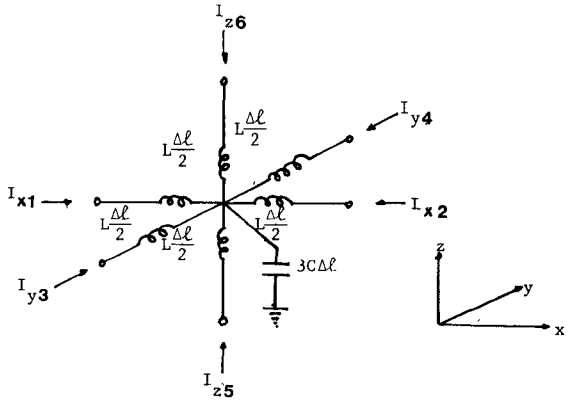

Fig. 19. Basic node of a three-dimensional scalar TLM network (after Choi and Hoefer [34]).

mesh. Errors and limitations are the same, and so are the possibilities of introducing losses and isotropic as well as anisotropic dielectric and magnetic materials.

D. The Scalar TLM Method

In those cases where electromagnetic fields can be decomposed into TE and TM modes (or LSE and LSM modes), it is only necessary to solve the scalar wave equation. Choi and Hoefer [34] have described a scalar TLM network to simulate a single field component or a Hertzian potential in three-dimensional space. The scalar TLM mesh can be thought of as a two-dimensional network to which additional transmission lines are connected orthogonally at each node as shown in Fig. 19. Such a structure could be realized in the form of a three-dimensional grid of coaxial lines.

The voltage impulses traveling across such a network represent the scalar variable to be simulated. Boundary reflection coefficients depend on both the nature of the boundary and that of the quantity to be simulated. For example, impulses will be subject to a reflection coefficient of -1 at a lossless electric wall if they represent either a tangential electric- or a normal magnetic-field component. A normal electric or a tangential magnetic field will be reflected with a coefficient of $+1$ in the same circumstances.

The slow-wave velocity in the three-dimensional scalar mesh is $c/\sqrt{3}$ as opposed to $c/2$ in the conventional TLM network. Dielectric or magnetic material as well as losses may be simulated using reactive and dissipative stubs.

The scalar method requires only 1/4 of the memory space and is seven times faster than the conventional method for a commensurate problem. However, its application is severely restricted, as it can be applied to scalar wave problems only.

VIII. Applications of the TLM Method

In the previous sections, the flexibility, versatility, and generality of the transmission-line matrix method has been demonstrated. In the following, an overview of potential applications of the method is given, and references describing specific applications are indicated. This list is not exhaustive, and many more applications can be found, not only in electromagnetism, but also in other fields dealing with wave phenomena, such as optics and acoustics.

For completeness, it should be mentioned that the TLM procedure can also be used to model and solve linear and nonlinear lumped networks [35]–[37] and diffusion problems [38]. Readers with a special interest in these applications should consult these references for more details.

Wave problems can be simulated in unbounded and bounded space, either in the time domain or—via Fourier analysis—in the frequency domain. Arbitrary homogeneous or inhomogeneous structures with anisotropic, space- and time-dependent electrical properties, including losses, can be simulated in two and three dimensions.

Below are some typical application examples.

A. Two-Dimensional Scattering Problems in Rectangular Waveguides (Field Distribution of Propagating and Evanescent Modes, Wave Impedance, Scattering Parameters)

- Open-circuited rectangular waveguide (TE_{n0}) [5].
- Bifurcation in rectangular waveguide (TE_{n0}) [5].
- Scattering by arbitrarily-shaped two-dimensional discontinuities in rectangular waveguide (TE_{n0}) including losses.

B. Two-Dimensional Eigenvalue Problems (Eigenfrequencies, Mode Fields)

- Cutoff frequencies and mode fields in homogeneous waveguides of arbitrary cross section, such as ridged waveguides [6], [8], [13], [26], [27].
- Cutoff frequencies and mode fields in inhomogeneous wavegudies of arbitrary cross section, such as dielectric loaded waveguides, finlines, image lines [7], [13], [16], [18], [21], [22], [25], [26], [28].

C. Three-Dimensional Eigenvalue and Hybrid Field Problems (Dispersion Characteristics, Wave Impedances, Losses, Eigenfrequencies, Mode Fields, Q-Factors)

- Characteristics of dielectric loaded cavities [10], [13], [14], [15], [18], [26], [27], [29], [32], [34].
- Dispersion characteristics and scattering in inhomogeneous planar transmission-line structures, including anisotropic substrate [11], [12], [13], [14], [17], [26], [27], [29], [30], [32].
- Transient analysis of transmission-line structures [19], [23], [33].

General-purpose two-dimensional and three-dimensional TLM programs can be found in Akhtarzad's Ph.D. thesis [13]. They can be adapted to most of the applications described above. If the various improvements and modifications described in Section VII are implemented in these programs, versatile and powerful numerical tools for the solution of complicated field problems are indeed obtained.

IX. Discussion and Conclusion

This paper has described the physical principle, the formulation, and the implementation of the transmission-line matrix method of analysis. Numerous features and applications of the method have been discussed, in particu-

lar the principal sources of error and their correction, the inclusion of losses, inhomogeneous and anisotropic properties of materials, and the capability to analyze transient as well as steady-state wave phenomena.

A general-purpose two-dimensional TLM program can be written in about 80 lines of FORTRAN, while a three-dimensional program is about 110 lines long. [13].

The method is limited only by the amount of memory storage required, which depends on the complexity of the structure and the nonuniformity of fields set up in it. In general, the smallest feature in the structure should at least contain three nodes for good resolution. The total storage requirement for a given computation can be determined by considering that each two-dimensional node requires five real number storage places, and an additional number equal to the number of iterations is needed to store the output impulse function. A basic three-dimensional node requires twelve number locations; if it is completely equipped with permittivity, permeability, and loss stubs, the required number of stores goes up to 26. Again, one real number must be stored per output function and per iteration. The number of iterations required varies between several hundred and several thousand, depending on the size and complexity of the TLM mesh.

As far as computational expenditure is concerned, the TLM method compares favorably with finite-element and finite-difference methods. Its accuracy is even slightly better by virtue of the Fourier transform, which ensures that the field function between nodes is automatically circular rather than linear as in the two other methods.

The main advantage of the TLM method, however, is the ease with which even the most complicated structures can be analyzed. The great flexibility and versatility of the method reside in the fact that the TLM network incorporates the properties of the electromagnetic fields and their interaction with the boundaries and materials. Hence, the electromagnetic problem need not to be reformulated for every new structure; its parameters are simply entered into a general-purpose program in the form of codes for boundaries, losses, permeability and permittivity, and excitation of the fields. Furthermore, by solving the problem through simulation of wave propagation in the time domain, the solution of large numbers of simultaneous equations is avoided. There are no problems with convergence, stability, or spurious solutions.

Another advantage of the TLM method resides in the large amount of information generated in one single computation. Not only is the impulse response of a structure obtained, yielding, in turn, its response to any excitation, but also the characteristics of the dominant and higher order modes are accessible in the frequency domain through the Fourier transform.

In order to increase the numerical efficiency and reduce the various errors associated with the method, more programing effort must be invested. Such an effort may be worthwhile when faced with the problem of scattering by a three-dimensional discontinuity in an inhomogeneous transmission medium, or when studying the overall electromagnetic properties of a monolithic circuit.

Finally, the TLM method may be adapted to problems in other areas such as thermodynamics, optics, and acoustics. Not only is it a very powerful and versatile numerical tool, but because of its affinity with the mechanism of wave propagation, it can provide new insights into the physical nature and the behavior of electromagnetic waves.

REFERENCES

[1] C. Huygens, "Traité de la Lumière" (Leiden, 1690).

[2] J. R. Whinnery and S Ramo, "A new approach to the solution of high-frequency field problems," *Proc. IRE*, vol. 32, pp. 284–288, May 1944.

[3] G. Kron, "Equivalent circuit of the field equations of Maxwell—I," *Proc. IRE*, vol. 32, pp. 289–299, May 1944.

[4] J. R. Whinnery, C. Concordia, W. Ridgway, and G. Kron, "Network analyzer studies of electromagnetic cavity resonators," *Proc. IRE*, vol. 32, pp. 360–367, June 1944.

[5] P. B. Johns and R. L. Beurle, "Numerical solution of 2-dimensional scattering problems using a transmission-line matrix," *Proc. Inst. Elec. Eng.*, vol 118, no. 9, pp. 1203–1208, Sept. 1971.

[6] P. B. Johns, "Application of the transmission-line matrix method to homogeneous waveguides of arbitrary cross-section," *Proc. Inst. Elec. Eng.*, vol. 119, no. 8, pp. 1086–1091, Aug. 1972.

[7] P. B. Johns, "The solution of inhomogeneous waveguide problems using a transmission-line matrix," *IEEE Trans. Microwave Theory Tech.*, vol. MTT-22, pp. 209–215, Mar. 1974.

[8] S. Akhtarzad and P. B. Johns, "Numerical solution of lossy waveguides: T.L.M. computer program," *Electron. Lett.*, vol. 10, no. 15, pp. 309–311, July 25, 1974.

[9] P. B. Johns, "A new mathematical model to describe the physics of propagation," *Radio Electron. Eng.*, vol. 44, no. 12, pp. 657–666, Dec. 1974.

[10] S. Akhtarzad and P. B. Johns, "Solution of 6-component electromagnetic fields in three space dimensions and time by the T.L.M. method," *Electron. Lett.*, vol. 10, no. 25/26, pp. 535–537, Dec. 12, 1974.

[11] S. Akhtarzad and P. B. Johns, "T.L.M. analysis of the dispersion characteristics of microstrip lines on magnetic substrates using 3-dimensional resonators," *Electron. Lett.*, vol. 11, no. 6, pp. 130–131, Mar. 20, 1975.

[12] S. Akhtarzad and P. B. Johns, "Dispersion characteristic of a microstrip line with a step discontinuity," *Electron. Lett.*, vol. 11, no. 14, pp. 310–311, July 10, 1975.

[13] S. Akhtarzad, "Analysis of lossy microwave structures and microstrip resonators by the TLM method," Ph.D dissertation, Univ. of Nottingham, England, July 1975.

[14] S. Akhtarzad and P.B. Johns, "Three-dimensional transmission-line matrix computer analysis of microstrip resonators," *IEEE Trans. Microwave Theory Tech.*, vol. MTT-23, pp. 990–997, Dec. 1975.

[15] S. Akhtarzad and P. B. Johns, "Solution of Maxwell's equations in three space dimensions and time by the T.L.M. method of analysis," *Proc. Inst. Elec. Eng.*, vol. 122, no. 12, pp. 1344–1348, Dec. 1975.

[16] S. Akhtarzad and P. B. Johns, "Generalized elements for T.L.M. method of numerical analysis," *Proc. Inst. Elec. Eng.*, vol. 122, no. 12, pp. 1349–1352, Dec. 1975.

[17] G. E. Mariki, "Analysis of microstrip lines on inhomogeneous anisotropic substrates by the TLM numerical technique," Ph.D. thesis, Univ. of California, Los Angeles, June 1978.

[18] W. J. R. Hoefer and A. Ros, "Fin line parameters calculated with the TLM method," in *IEEE MTT Int. Microwave Symp. Dig.* (Orlando, FL), Apr. 28–May 2, 1979.

[19] N. Yoshida, I. Fukai, and J. Fukuoka, "Transient analysis of two-dimensional Maxwell's equations by Bergeron's method," *Trans. IECE Japan*, vol. J62B, pp. 511–518, June 1979.

[20] P. Saguet and E. Pic, "An improvement for the TLM method," *Electron. Lett.*, vol. 16, no. 7, pp 247–248, Mar. 27, 1980.

[21] Y.-C. Shih, W. J. R. Hoefer, and A. Ros, "Cutoff frequencies in fin lines calculated with a two-dimensional TLM-program," in *IEEE MTT Int. Microwave Symp. Dig.* (Washington, DC), June 1980, pp. 261–263.

[22] W. J R. Hoefer and Y.-C. Shih, "Field configuration of fundamental and higher order modes in fin lines obtained with the TLM method," presented at URSI and Int. IEEE-AP Symp., Quebec, Canada, June 2–6, 1980.

[23] N. Yoshida, I. Fukai, and J. Fukuoka, "Transient analysis of three-dimensional electromagnetic fields by nodal equations," *Trans. IECE Japan*, vol. J63B, pp. 876–883, Sept. 1980.
[24] A. Ros, Y.-C. Shih, and W. J. R. Hoefer, "Application of an accelerated TLM method to microwave systems," in *10th Eur. Microwave Conf. Dig.* (Warszawa, Poland), Sept. 8–11, 1980, pp. 382–388.
[25] Y.-C. Shih and W. J. R. Hoefer, "Dominant and second-order mode cutoff frequencies in fin lines calculated with a two-dimensional TLM program," *IEEE Trans. Microwave Theory Tech.*, vol. MTT-28, pp. 1443–1448, Dec. 1980.
[26] Y.-C. Shih, "The analysis of fin lines using transmission line matrix and transverse resonance methods," M.A.Sc. thesis, Univ. of Ottawa, Canada, 1980.
[27] D. Al-Mukhtar, "A transmission line matrix with irregularly graded space," Ph.D. thesis, Univ. of Sheffield, England, Aug. 1980.
[28] P. Saguet and E. Pic, "Le maillage rectangulaire et le changement de maille dans la méthode TLM en deux dimensions," *Electron. Lett.*, vol. 17, no. 7, pp. 277–278, Apr. 2, 1981.
[29] D.A. Al-Mukhtar and J. E. Sitch, "Transmission-line matrix method with irregularly graded space," *Proc. Inst. Elec. Eng.*, vol. 128, pt. H, no. 6, pp. 299–305, Dec. 1981.
[30] N. Yoshida, I. Fukai, and J. Fukuoka, "Application of Bergeron's method to anisotropic media," *Trans. IECE Japan*, vol J64B, pp. 1242–1249, Nov. 1981.
[31] P. Saguet and E. Pic, "Utilisation d'un nouveau type de noeud dans la méthode TLM en 3 dimensions," *Electron. Lett.*, vol. 18, no. 11, pp. 478–480, May 1982.
[32] P. Saguet, "Le maillage parallelepipédique et le changement de maille dans la méthode TLM en trois dimensions," *Electron. Lett.*, vol. 20, no. 5, pp. 222–224, Mar. 15, 1984.
[33] N. Yoshida and I. Fukai, "Transient analysis of a stripline having a corner in three-dimensional space," *IEEE Trans. Microwave Theory Tech.*, vol. MTT-32, pp. 491–498, May 1984.
[34] D. H. Choi and W. J. R. Hoefer, "The simulation of three-dimensional wave propagation by a scalar TLM model," in *IEEE MTT Int. Microwave Symp. Dig.* (San Francisco), May 1984.
[35] P. B. Johns, "Numerical modelling by the TLM method," in *Large Engineering Systems*, A. Wexler, Ed. Oxford: Pergamon Press, 1977.
[36] J. W. Bandler, P. B. Johns, and M. R. M. Rizk, "Transmission-line modeling and sensitivity evaluation for lumped network simulation and design in the time domain," *J. Franklin Inst.*, vol. 304, no. 1, pp. 15–23, 1977.
[37] P. B. Johns and M. O'Brien, "Use of the transmission-line modelling (T.L.M.) method to solve non-linear lumped networks," *Radio Electron. Eng.*, vol. 50, no. 1/2, pp. 59–70, Jan./Feb. 1980.
[38] P. B. Johns, "A simple explicit and unconditionally stable numerical routine for the solution of the diffusion equation," *Int. J. Num. Meth. Eng.*, vol. 11, pp. 1307–1328, 1977.

✠

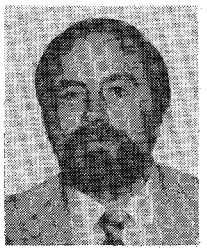

Wolfgang J. R. Hoefer (M'71–SM'78) was born in Urmitz/Rhein, Germany, on February 6, 1941. He received the diploma in electrical engineering from the Technische Hochschule Aachen, Aachen, Germany, in 1964, and the D. Ing. degree from the University of Grenoble, Grenoble, France, in 1968.

After one year of teaching and research at the Institut Universitaire de Technologie, Grenoble, France, he joined the Department of Electrical Engineering, University of Ottawa, Ottawa, Ontario, Canada, where he is currently a Professor. His sabbatical activities included six months with the Space Division of the AEG-Telefunken in Backnang, Germany, six months with the Electromagnetics Laboratory of the Institut National Polytechnique de Grenoble, France, and one year with the Space Electronics Directorate of the Communications Research Centre in Ottawa, Canada. His research interests include microwave measurement techniques, millimeter-wave circuit design, and numerical techniques for solving electromagnetic problems.

Dr. Hoefer is a registered Professional Engineer in the province of Ontario, Canada.